AIAA/AAS Astrodynamics Specialist Conference and Exhibit
5-8 August 2002, Monterey, California

AIAA 2002-4888

DYNAMIC CALIBRATION ATMOSPHERE (DCA) FOR THE HIGH ACCURACY SATELLITE DRAG MODEL (HASDM)

Stephen J. Casali
AIAA Member, Astrodynamicist
Omitron Inc., Colorado Springs, CO

William N. Barker
AIAA Senior Member, Chief Scientist for Astrodynamics
Omitron Inc., Colorado Springs, CO

Abstract

The Dynamic Calibration Atmosphere (DCA) represents Phase I of the High Accuracy Satellite Drag Model (HASDM) initiative. DCA uses tracking data on a set of calibration satellites to determine corrections to the Jacchia 70 density model in near real-time. The density corrections take the form of spherical harmonic expansions of two Jacchian temperature parameters that enhance spatial resolution. This paper describes the DCA solution over the first half of 2001 and its application to forty evaluation satellites. Improvements due to DCA in ballistic coefficient consistency, epoch accuracy, and epoch covariance realism are measured and demonstrated.

Introduction

Applied density models have changed little since the 1970s. They generally suffer from poor inputs as well as low temporal and spatial resolution. Their inputs consist of crude heating indices, namely the familiar $F_{10.7}$, its 81-day average, and a_p. The former ($F_{10.7}$ and its average) is a solar radio flux measure loosely correlated with the true extreme ultraviolet (EUV) heating of the thermosphere. The latter (a_p) is a measure of geomagnetic activity that serves as an indicator of atmospheric Joule heating. The overall model imprecision seriously limits the orbital accuracy attained for most Low Earth Orbit (LEO) satellites, particularly those below about 600 km altitude.

Recently, AFSPC/ASAC and Omitron Inc. have undertaken the challenge to make improvements to the Jacchia 70 density model through an initiative known as the High Accuracy Satellite Drag Model (HASDM), sponsored by the Air Force Space Battlelab. The Dynamic Calibration Atmosphere (DCA) represents Phase I of this effort. DCA is an attempt to improve the density field in near real-time by observing drag effects on a set of LEO calibration satellites receiving abundant Space Surveillance Network (SSN) tracking data. Many calibration satellites are exploited to recover a dynamically responsive density field with improved spatial resolution. The satellites are chosen so as to encompass a wide range of orbital altitudes, inclinations, and ascending nodes. Only those satellites with reasonably constant frontal area are considered.

The solved-for density field actually consists of corrections to the Jacchia 70 density model[1] via an expanded model called J70DCA, developed by AFSPC/ASAC.[2] J70DCA effects change in density through dynamic temperature field modifiers expressible as spherical harmonic expansions of two Jacchian temperature parameters. The parameter choice and spherical harmonic form allow for increased density fidelity in latitude, longitude and height.

DCA Approach

Fundamentally, DCA makes corrections to select parameters of a density model. The corrections are determined in a single weighted differential correction (DC) across all the calibration satellites using their observations and statistical uncertainties directly, while simultaneously solving for their states. This is in contrast to other methods that perform satellite-by-satellite solutions using indirect observations synthesized from particular behaviors (e.g., ballistic coefficient histories).

There are several potential advantages to this direct approach. First, it is theoretically optimal from an estimation standpoint. Second, uncertainties and correlations of the solution set are a natural by-product. Third, diverse data sets can be included seamlessly (e.g., satellite radar data mixed with future accelerometer data). Fourth, the problem of producing satellite-specific solutions and then assimilating them into a global representation is avoided. Finally, the approach lends itself to near real-time application, being conceptually similar to the way other DCs are normally performed.

The DCA state (X), consisting of all solve-for parameters, is defined as:

$$X^T = \begin{bmatrix} X_1^T & X_2^T & \cdots & X_N^T & X_D^T \end{bmatrix}$$

where X_i represents the i^{th} satellite state (i=1 thru N);
X_D represents the set of density corrections.

The DCA solution for the corrections (ΔX) is given by:

$$\begin{bmatrix} (A^TWA)_1 & 0 & 0 & \cdots & (A^TWD)_1 \\ 0 & (A^TWA)_2 & 0 & \cdots & (A^TWD)_2 \\ 0 & 0 & \ddots & \vdots & \vdots \\ \vdots & \vdots & \cdots & (A^TWA)_N & (A^TWD)_N \\ (D^TWA)_1 & (D^TWA)_2 & \cdots & (D^TWA)_N & (D^TWD)_\Sigma \end{bmatrix} \Delta X = \begin{bmatrix} (A^TWb)_1 \\ (A^TWb)_2 \\ \vdots \\ (A^TWb)_N \\ (D^TWb)_\Sigma \end{bmatrix}$$

where A denotes partials matrices relating satellite state variables to observations;
D denotes partials matrices relating density parameters to observations;
W denotes observation weight matrices;
b denotes residual vectors.

As with the state definition, the subscripts 1 thru N in the solution matrices denote individual satellite entries, and the two blocks with summation sign subscripts (D^TWD and D^TWb) imply accumulation over all satellites. Note that the left-hand-side matrix is sparse, as individual satellite states are uncoupled. This greatly simplifies the matrix inversion needed to obtain ΔX, as standard formulas for partitioned matrices can be employed that allow inversion of just the diagonal blocks for the sparse portion of the matrix.

Since the resolution of the density corrections is significantly greater than the observational data span needed to achieve the state solutions, a "segmented" approach is employed in the estimation for the DCA parameters. The DCA segments (1 through n) and their associated density corrections (d_i) across the DCA span can be visualized as:

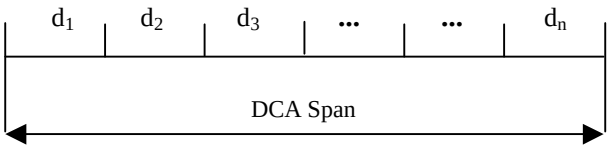

DCA Solution

Sixty calibration satellites were used to calibrate a temperature correction field over the first half of 2001. The satellites were selected based on their similar ballistic coefficient (B) histories over 2000-2001 (as an indicator of frontal area stability) and on their variety of orbital altitudes, inclinations, and ascending nodes. Their attributes are given in Table 1 (following page), which is sorted by energy dissipation rate (EDR), a measure of the amount of drag acting on a satellite. Greatly increased sensor tasking and response from the SSN was obtained on all 60 satellites.

First, experimental work was necessary to determine the optimal configuration of DCA and J70DCA in terms of their solution parameters. J70DCA models two temperature parameters, an exospheric temperature parameter and an inflection temperature parameter, per a specified degree and order spherical harmonic expansion (up to a 6x6 field). DCA performs regular solutions on a segmented basis for global density parameters in conjunction with the states of the individual satellites over a specified time period, the DCA span. The optimization task was to determine a suitable degree and order for the temperature parameters of J70DCA at an acceptable temporal resolution within DCA, while maintaining adequate SSN observability across the calibration satellites.

The optimization task was complicated by imprecise knowledge of the "true" B values across the calibration set in general. In this regard, AFSPC/ASAC performed a 30-year average-B analysis to provide good starting values for 23 of the satellites, as well as produce estimates for the remaining 37 true B values derived from their 180-day study averages. As described later, all the true B values were adjusted during the solution process.

The answer to the optimization task was not obvious, of course. However, there was some initial idea as to what was achievable and what to aspire toward. For example, it was thought that at least a 2×2 field should be attempted to adjust and modulate the strong diurnal component already present in the Jacchia 70 model, as well as introduce a diurnal feature. For a single temperature parameter, say exospheric temperature, a 2×2 field consists of 9 coefficients per DCA segment. That would seem well within the capacity of DCA to estimate from a 60-satellite constellation, if one conceptually thinks of each satellite and its SSN dataset as collapsing into approximately one observable (at a minimum) of the temperature field.

Increasing the resolution to a 3×3 field increases the number of coefficients to 16 per segment, which still seems sensible. However, considering there are actually two temperature fields, and that the true B values themselves are not precisely known or quite constant (which can markedly affect the solution), it was not clear how much observability of a 3×3 field could actually be attained from just 60 satellites.

Table 1 – Calibration Satellites

Entry	Object Type	EDR (watts/kg)	B (m2/kg)	Period (min)	Inclination (Deg)	Apogee (Km)	Perigee (Km)
1	R/B	0.0007	0.044	99.9	98.3	892	614
2	P/L	0.0011	0.199	101.0	69.9	814	801
3	P/L+R/B	0.0012	0.032	97.7	98.2	669	635
4	R/B	0.0015	0.076	98.6	98.2	716	675
5	P/L	0.0015	0.016	96.0	81.2	583	556
6	P/L	0.0017	0.016	95.9	81.1	564	559
7	P/L	0.0017	0.014	95.7	48.5	579	526
8	P/L	0.0018	0.230	100.3	70.0	780	771
9	P/L	0.0018	0.016	95.7	81.2	564	547
10	P/L	0.0019	0.017	95.9	81.1	568	554
11	P/L	0.0019	0.018	96.0	97.5	583	555
12	P/L	0.0020	0.013	95.3	81.2	539	534
13	R/B	0.0021	0.020	97.6	35.6	812	470
14	P/L	0.0021	0.011	95.0	53.0	526	513
15	R/B	0.0021	0.050	97.4	47.9	650	620
16	R/B	0.0022	0.012	95.2	81.2	548	508
17	DEB	0.0023	0.448	101.6	99.7	872	801
18	DEB	0.0023	0.476	102.0	98.8	908	803
19	P/L	0.0024	0.011	103.7	82.9	1483	384
20	R/B	0.0024	0.013	95.2	81.2	545	510
21	P/L	0.0024	0.011	103.3	83.0	1448	382
22	P/L	0.0024	0.035	96.8	98.6	613	605
23	DEB	0.0025	0.885	102.4	100.1	889	856
24	DEB	0.0025	0.616	101.9	66.9	902	800
25	R/B	0.0026	0.018	95.5	97.6	565	521
26	P/L	0.0027	0.005	93.4	87.3	470	415
27	P/L	0.0028	0.016	104.8	82.5	1574	393
28	P/L	0.0028	0.021	96.3	98.1	676	491
29	P/L	0.0029	0.015	102.0	74.0	1326	384
30	P/L	0.0032	0.016	95.1	97.7	546	507
31	P/L	0.0037	0.021	108.4	102.7	1931	373
32	P/L	0.0040	0.022	95.2	93.4	558	504
33	R/B	0.0051	0.018	102.4	82.9	1377	363
34	P/L	0.0054	0.023	100.1	49.9	1143	386
35	R/B	0.0054	0.051	96.2	48.3	597	555
36	R/B	0.0059	0.024	96.7	46.0	777	418
37	R/B	0.0061	0.042	95.7	98.2	605	507
38	R/B	0.0061	0.017	98.5	82.9	1015	360
39	P/L	0.0062	0.019	95.0	74.0	608	433
40	DEB	0.0069	0.358	99.2	98.5	723	716
41	P/L	0.0071	0.013	94.0	38.0	492	444
42	R/B	0.0071	0.017	97.6	74.0	942	349
43	P/L	0.0085	0.012	93.7	64.9	493	418
44	R/B	0.0098	0.031	95.0	81.7	570	467
45	P/L	0.0108	0.016	96.1	73.9	810	340
46	R/B	0.0108	0.019	95.2	45.0	665	394
47	DEB	0.0114	0.012	93.4	65.8	453	429
48	R/B	0.0115	0.019	100.1	52.2	1199	326
49	R/B	0.0116	0.021	95.4	41.0	713	359
50	R/B	0.0138	0.020	100.2	25.8	1210	327
51	DEB	0.0169	0.252	97.7	98.7	653	647
52	R/B	0.0178	0.012	93.1	81.2	446	410
53	R/B	0.0178	0.018	94.3	97.0	597	374
54	R/B	0.0184	0.019	102.4	23.0	1445	302
55	DEB	0.0235	0.041	94.6	97.5	519	485
56	DEB	0.0235	0.199	97.3	99.9	669	589
57	DEB	0.0248	0.230	97.4	98.8	661	610
58	R/B	0.0251	0.012	93.0	81.2	436	412
59	DEB	0.0345	0.051	95.7	66.0	701	406
60	DEB	0.0512	0.127	97.5	62.8	832	442

From the beginning, fields higher than 3×3 were not seriously considered, and the consensus was that either a 2×2 or a 3×3 field was the most logical starting point for either or both temperature parameters.

Regarding the temporal resolution of the field, a 3-hourly variation was desirable because that is the resolution of the current Jacchia temperature model, upon which the corrections are made. However, limitations are imposed by the SSN coverage and the accuracy of the data returned, so the implications for 3-hour resolution were not obvious even for the low degree and order fields under consideration.

Solution Experimentation

With these considerations in mind, experimental DCA runs were conducted over approximately a dozen DCA spans chosen throughout the 180-day study period. The DCA spans themselves were chosen between 1.5 days and 3 days based on previous experience that these relatively short spans give good state observability for the level of SSN tasking in place, without reaching a point of diminishing returns or incurring excessive mis-modeling, as experienced by longer spans. The full state for each satellite was estimated, with the ballistic coefficient receiving appropriate *a priori* information consistent with its inherent uncertainty of a few percent (a combination of uncertainty in the true B, localized density errors, and frontal area variation).

The primary metrics of interest from the DCA runs were the weighted RMS (root-mean-square) of the fits and the covariance-derived uncertainties of the solve-for temperature parameters. The former was used to determine goodness of fit, or the level to which the SSN data was fit relative to its calibrated weights. The latter was needed to gauge confidence of fit. These were supplemented by monitoring the convergence behavior for robustness of solution.

From this set of experimental runs, it was immediately clear that an entire 2×2 or 3×3 temperature field could not be satisfactorily observed at a 3-hour resolution. However, the zeroeth-degree term could be acceptably observed at a 3 to 6-hour resolution, depending on the level of solar activity. During periods of higher activity, 3 hours was achievable and required to adequately fit the data, while during periods of lower activity, 3-hour resolution was more difficult to achieve and did not provide significant improvement over a 6-hour resolution. Furthermore, the 2×2 field demonstrated improved fitting capability over just a zeroeth-degree field, but required longer DCA segments of 12-24 hours. The efficacy of using a 3×3 field was not clearly established with these initial runs, as it improved the fits only marginally over a 2×2 field.

These experimental results generally held true regardless of which temperature parameter was invoked. Attempting to solve for the two fields simultaneously presented additional observability problems. While the zeroeth-degree term of the inflection temperature field showed merit in "synchronizing" the temperature profile across the height regime of the calibration constellation, the higher-order terms of the field were not separable from the higher-order terms of the exospheric temperature field. Moreover, even the zeroeth-degree terms of both fields could not be solved for simultaneously at less than a 6 to 12-hour resolution. These results probably suggest a less than optimal sampling of perigee heights within the calibration constellation. Therefore, higher-order coefficients were only retained in the exospheric temperature field for the study. This situation was later remedied as described at the end of the paper.

At this point, it became clear that DCA needed the capability to solve for different parameters at different temporal resolutions to achieve the original goal of supporting a 2×2 exospheric temperature field with inflection temperature adjustment, while also making corrections on a 3-hourly basis. These capabilities were added, and the experimental runs were reaccomplished and revalidated more completely, though it was still unclear how much benefit was gained from a 3×3 temperature field over a 2×2 field.

Final Solution

After the above experiments had been completed, the DCA solutions were extended to the full 180 days. Using the experimental runs as a guide, a final set of test runs was conducted across the whole study interval to arrive at a continuous temperature field and better ascertain the improvements of a 3×3 field. In addition to the previously described metrics, these runs also looked at the variability of the solved-for ballistic coefficient histories over the 180 days to help discriminate between solutions.

Specifically, the final runs were constructed as follows: The DCA span was set to 1.5 days; the zeroeth-degree exospheric temperature coefficient was solved for every 3 hours; the higher-order exospheric temperature coefficients were solved for every 18 hours; a zeroeth-degree inflection temperature field was also solved for every 18 hours; and the *a priori* uncertainty for the true B values was set to 3% (RMS).

Midway through this set of tests, it was discovered that finer resolution of the solved-for Bs was

required for some of the high EDR satellites over periods of elevated solar activity to properly account for satellite-dependent effects. These effects consist of an inseparable combination of localized density errors (that part "left-over" from the global J70DCA representation) and varying frontal area. Therefore, local density compensators (or LDCs) were introduced into DCA to control these unwanted errors via a super-imposed segmented B solution by satellite. A 3-hour segmentation was sufficient in conjunction with an *a priori* uncertainty of 3% (RMS), as is consistent with the best level of drag modeling thought to be statistically attainable by DCA.

With this DCA configuration, the final runs were performed for both the 2×2 and 3×3 exospheric temperature fields. Each solution produced the same high quality fit to the SSN data in terms of their weighted RMS histories (each lay about unity, with one history virtually indistinguishable from the other), but they gave slightly different B variations. While both solutions performed satisfactorily in this respect, giving B variations of just a few percent RMS, the 3×3 solution was a little better. However, the uncertainties of the temperature coefficients were generally higher for the 3×3 solution, and the solution was less robust, raising questions of extendibility to non-calibration satellites. Therefore, the 2×2 field was chosen for the DCA evaluation.

DCA Evaluation

Forty evaluation satellites (not included in the temperature field solution, of course) on increased SSN tasking were used to assess the improvement afforded by DCA. Their attributes are given in Table 2 (following page). The B histories over 2000-2001 for these satellites were generally not as consistent as they were for the calibration satellites. Based on B behavior, they were classified into two groups: typical and difficult satellites.

The typical satellites (entries 61-88 of Table 2, sorted by EDR) were not overly dissimilar from the calibration satellites in their B histories, and are thought to represent the majority of the drag catalog. The difficult satellites (entries 89-100 of Table 2, sorted by EDR), on the other hand, were purposely selected for the evaluation because they generally did *not* follow apparent B trends as exhibited by the other satellites. Inclusion of these satellites was intended to help reveal limitations of DCA imposed by varying frontal area and/or localized density anomalies. A few of them in particular are payloads known to exhibit large frontal area variation through attached solar panels and/or long antennae.

For the sake of completeness, the DCA solution was also applied to the calibration satellites as well as the evaluation satellites. The "DCA-applied" case was compared, satellite-by-satellite, to a "baseline" case that did not apply DCA to assess improvement. The metrics of interest were B consistency, epoch accuracy, and covariance realism, all measured statistically over the 180-day study interval in the context of batch weighted DC output. This, of course, implied a means of measuring these. (Prediction accuracy, which entails solar forecasting, is not addressed until Phase II of HASDM.)

Epoch accuracy and covariance realism were evaluated through established reference orbit building techniques that perform statistical reduction on the abutment error between the many separate ephemerides that comprise a long-term reference orbit. These ephemerides actually overlap by plus and minus half an orbit revolution on either side of the nominal abutments, producing a large sample of abutment errors over a reference orbit span. Each abutment error is computed in terms of UVW (radial, transverse, and normal) components, considering both actual error and error relative to its covariance estimate. The former, of course, measures absolute error, while the latter assesses covariance realism by looking at the residuals in a normalized sense, seeking a standard deviation (STD) of unity (similar to a weighted RMS in a DC). The number of nominal abutments going into the statistical reduction depends on the reference orbit span, the orbit determination interval (ODI) for each ephemeris, and the amount of observational data overlap between adjacent ephemerides.

For this analysis, the ODIs ranged from 1 to 3 days, predominantly 1.5 days, and the observational data overlap was ½, meaning the ephemeris spanned the middle half of the ODI. (The statistical implications of overlapping the data in this way are a little off the subject, but practically, the individual ephemerides of the reference orbits should be bounded on either end by observational data.) For the 1.5-day ODIs, this meant that each reference orbit, spanning 180 days, was comprised of 240 ephemerides, giving rise to 239 nominal abutments (each with an orbit revolution's worth of abutment errors). The statistics of these abutments and the solved-for B values from each DC are the metrics used in this section to measure epoch accuracy, covariance realism, and B consistency. In the case of epoch accuracy and covariance realism, only the vector magnitude (VMAG) of the UVW errors is presented for conciseness.

Table 2 – Evaluation Satellites

Entry	Object Type	EDR (watts/kg)	B (m2/kg)	Period (min)	Inclination (Deg)	Apogee (Km)	Perigee (Km)
61	P/L	0.0005	0.010	111.1	68.4	2123	431
62	P/L	0.0009	0.022	98.0	50.3	813	515
63	DEB	0.0011	0.302	101.6	98.6	859	811
64	P/L	0.0012	0.033	97.8	98.3	659	650
65	R/B	0.0016	0.020	97.8	35.6	829	475
66	DEB	0.0021	0.014	101.5	66.1	1261	402
67	DEB	0.0022	0.882	103.6	100.0	956	901
68	R/B	0.0025	0.019	110.6	25.0	2114	394
69	R/B	0.0029	0.009	96.1	78.9	753	397
70	R/B	0.0030	0.016	103.3	83.0	1438	391
71	R/B	0.0031	0.014	100.9	74.0	1230	378
72	R/B	0.0040	0.016	101.4	82.9	1284	369
73	P/L	0.0046	0.015	110.4	82.1	2165	322
74	R/B	0.0048	0.020	100.0	25.3	1128	382
75	R/B	0.0052	0.010	93.7	64.0	543	372
76	P/L	0.0083	0.016	94.0	81.2	474	468
77	DEB	0.0086	0.252	98.7	98.9	730	665
78	P/L	0.0093	0.008	99.9	83.0	1226	289
79	P/L	0.0095	0.016	95.0	78.9	654	381
80	P/L	0.0098	0.016	93.8	81.2	465	463
81	DEB	0.0114	0.110	99.1	62.6	967	465
82	P/L	0.0115	0.008	99.1	82.9	1145	284
83	DEB	0.0131	0.253	97.7	98.3	665	637
84	DEB	0.0151	0.111	97.9	62.3	832	484
85	DEB	0.0158	0.135	101.1	79.8	1163	457
86	R/B	0.0159	0.019	99.6	52.3	1163	312
87	DEB	0.0223	0.153	97.7	62.3	804	493
88	DEB	0.0357	0.307	97.5	98.7	645	640
89	P/L	0.0010	0.756	105.0	90.0	1029	959
90	DEB	0.0019	0.095	98.7	74.0	714	680
91	P/L	0.0019	0.015	95.6	81.2	555	544
92	P/L	0.0023	0.029	96.9	65.0	701	521
93	P/L	0.0024	0.016	95.4	81.2	550	530
94	P/L	0.0024	0.012	95.0	81.2	527	512
95	P/L	0.0043	0.013	94.4	81.2	505	476
96	DEB	0.0058	0.207	98.2	98.1	690	659
97	DEB	0.0060	0.102	99.6	56.1	976	499
98	DEB	0.0062	0.454	99.7	70.0	784	710
99	DEB	0.0090	0.042	95.3	98.6	536	535
100	P/L	0.0126	0.026	94.7	97.7	508	503

Evaluation Results

Figure 1 shows the statistics of the B values for the baseline and DCA cases computed over the entire 180-day study period. The bars showing the solution sigmas for B (i.e., their theoretical population standard deviations) are given for reference sake, as representing "best case" given the statistical uncertainty in the SSN observational data. This is the level attainable if the dynamic model (including DCA) were perfect and the only remaining error source were that of the sensor measurements

In Figure 1, for the calibration satellites, DCA reduced the average B variation from 16.2% to 4.3%. For the typical evaluation satellites, DCA reduced the average B variation from 16.3% to 7.4%, while the corresponding reduction for the difficult evaluation satellites was from 21.6% to 13.3%.

Note that cases 61 and 62 show little improvement primarily because of low drag observability, as evidenced by the elevated bars on solution sigma. Cases 68 and 70 show similar tendencies. These cases could be improved with longer ODIs, but the overall indication is that they are not affected enough by drag to be substantially improved by DCA. However, drag is not a dominant source of error for these satellites in the first place, so these cases do not represent a major concern, though they artificially inflate the evaluation statistics somewhat (for both the baseline and DCA cases). These cases indirectly indicate that, not surprisingly, there exists a lower limit on EDR below which a satellite will not contribute measurably to the DCA solution (or be affected by it); a finding of relevance to the selection of calibration satellites.

Several cases in the difficult evaluation satellite category (starting at entry 89) stand out for their conspicuously elevated B variations, both in the baseline and DCA cases. Recall that these satellites were chosen specifically for their difficulty. Of the four DCA cases above the 15% level, one was a payload (entry 95) undergoing frontal area variation caused by large solar panels, and another was also a payload (entry 89) that, in addition to having an altitude of 1000 km, possesses several protruding 40-foot antennae. The remaining two satellites are pieces of debris susceptible to frontal area variability.

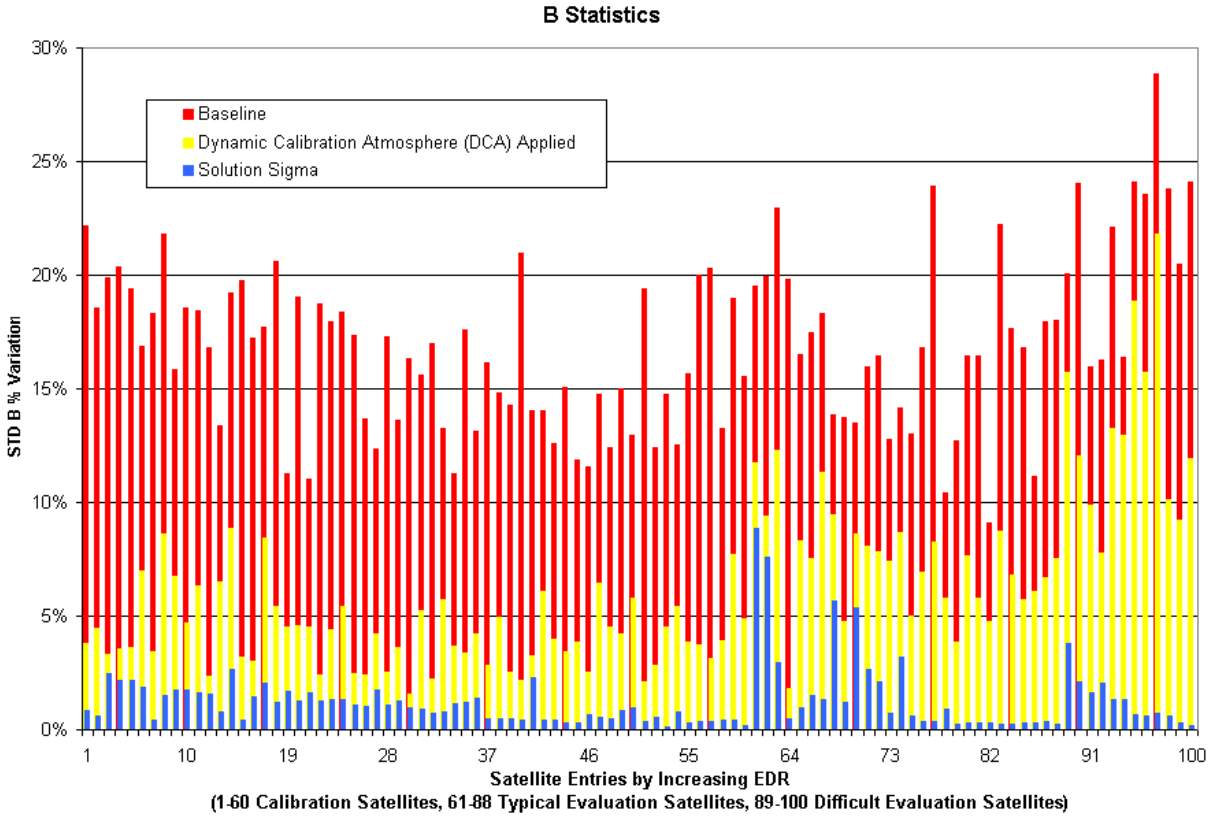

Figure 1 – B Statistics

Figure 2 shows the relative epoch accuracy estimates resulting from the reference orbit building process, as described at the beginning of the section. The vertical axis has been arbitrarily scaled from 0 to 100. "Segmented Solution for B (SSB)" refers to batch weighted DCs that perform high-frequency B solutions. It used 3-day ODIs and was included for the sake of reference as representing the near best that could be expected for epoch accuracy and covariance realism.

In Figure 2, for the calibration satellites, the average errors are about 27, 17 and 10 for the baseline, DCA, and SSB cases, respectively. For the typical evaluation satellites, the corresponding average errors are about 33, 23, and 12, while for the difficult evaluation satellites, they are 27, 18, and 10. While the STDs on these figures are high, due primarily to the wide range of EDRs under evaluation (and partly due to some disparity in tracking among the satellites), the DCA case exhibits less variability than the baseline case.

Curiously, the difficult satellites show better epoch accuracies than the typical satellites. This is not a contradiction, however, because the difficult satellites were not chosen in terms of epoch accuracy considerations, but in terms of B history behavior. As a group, their EDRs are actually lower than those of the typical evaluation group (reference Table 2), so their epoch accuracies are better.

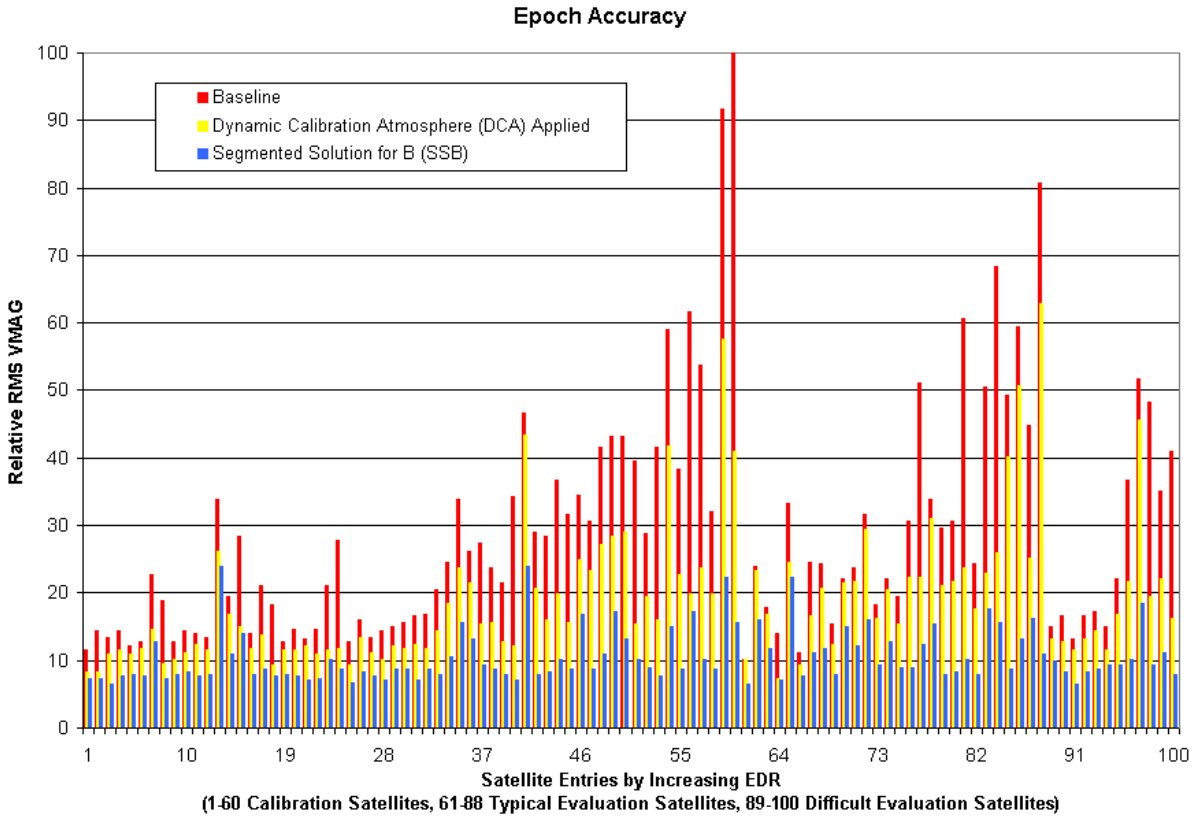

Figure 2 – Epoch Accuracy

Figure 3 shows the epoch covariance realism resulting from the reference orbit building process, as described at the beginning of the section. Recall that a value of unity is ideal for this measure. Again, the SSB case has been shown for reference. Note the results for this case are near optimal, with the bars coming in near unity except for a couple of satellites.

In Figure 3, for the calibration satellites, the averages of the normalized errors are about 2.04, 1.31, and 0.87 for the baseline, DCA, and SSB cases, respectively. For the typical evaluation satellites, the corresponding averages are about 2.55, 1.91, and 0.95, while for the difficult satellites, they are 2.56, 1.87, and 0.99.

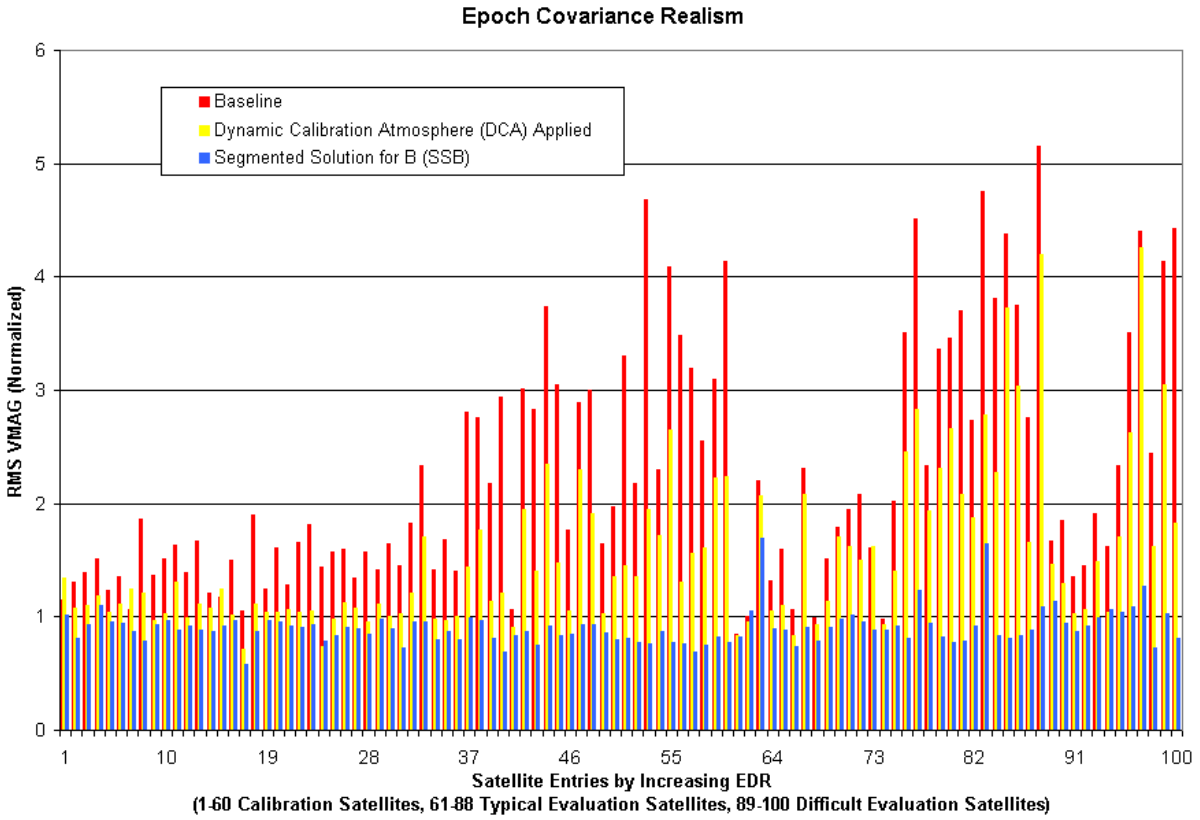

Figure 3 - Epoch Covariance Realism

Finally, Figure 4 (following page) shows sample B time-histories as were used to form the bars in Figure 1. Specifically, these correspond to entries 87, 94 and 64, respectively, and all are evaluation satellites. The first represents rather typical performance for the evaluation satellites with a reduction in the percent change in B from about 17% to about 6% (STD). The second shows a reduction of 18% to 13%, with the difference in performance attributed to evidently changing frontal area from about day 80 to day 150. The last example represents the best of the evaluation satellites with a reduction from about 20% to about 3%. Note that DCA performed well over days 75 through 105, over which time numerous large geomagnetic storms occurred.

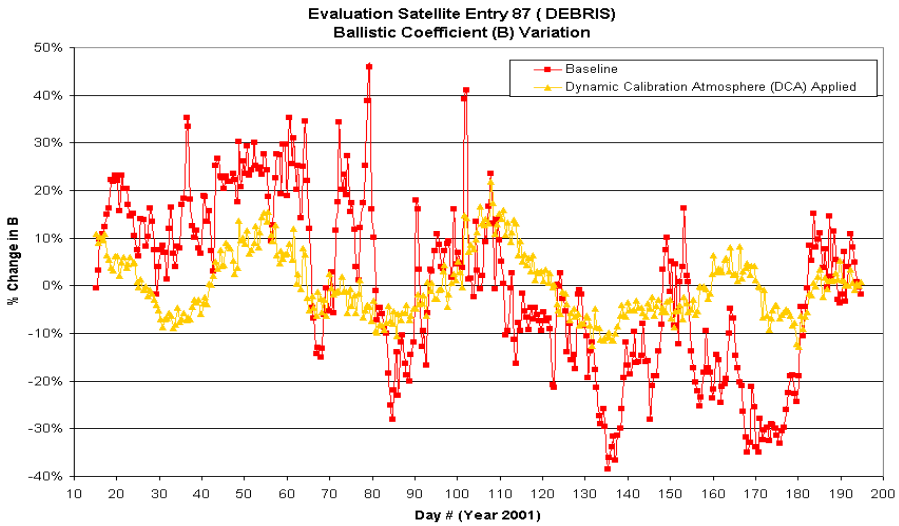

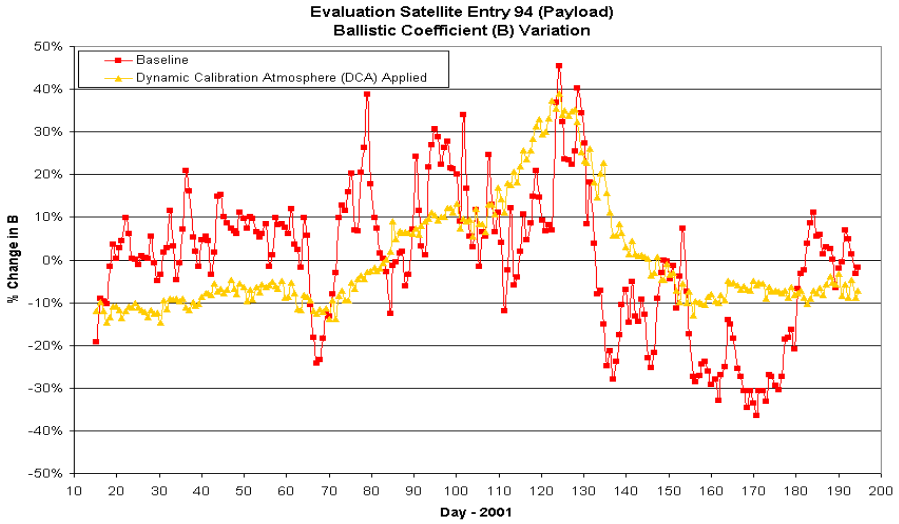

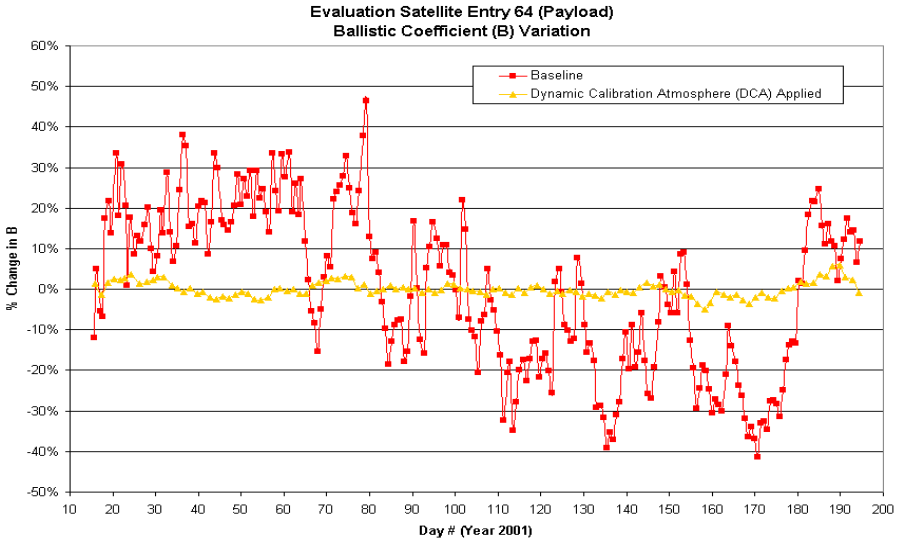

Figure 4 – Sample B Histories from the Evaluation Satellites

Conclusions

The primary objective of DCA at this developmental stage, i.e., as representing Phase I of HASDM, is improving the state accuracy at epoch (prediction accuracy is not addressed until Phase II). A related measure of success is enhanced realism of the state covariance at epoch. A third essential criterion is a demonstrated reduction in density error over time as measured by better consistency in ballistic coefficient.

The results of this study are favorable for all three measures. Epoch accuracy, covariance realism, and ballistic coefficient consistency were all improved for every satellite studied, some dramatically so. As such, DCA was judged to be feasible and demonstrates good operational potential.

Of course, it is a given that DCA must be operationally viable in addition to demonstrating scientific feasibility. This consideration was taken into account with the practical choice of the starting software. The viability was further ensured by the favorable CPU performance realized in the solution phase, with DCA updates taking less than 10 minutes on a computer less capable than the current operational hardware. These favorable CPU results also demonstrate the feasibility of expanding the 60-satellite calibration constellation without incurring excessive CPU burden. Lastly, operational viability was solidified through exhaustive use of the prototypical software in the solution and evaluation phases, which required processing large amounts of real tracking data.

Finally, though promising, it is clear that DCA alone is not the final solution. For example, while the 75% reduction in ballistic coefficient variation (from about 16% to 4%) over the calibration satellites is definitely encouraging, the approximately 50% reduction across the evaluation satellites is not optimal. Furthermore, for epoch accuracy and covariance realism, DCA falls about halfway between the baseline and SSB case, which, though representing a significant improvement, is also not ideal. Therefore, to maximize operational benefit, it will probably be necessary to use SSB in conjunction with DCA for moderate to high EDR satellites to control satellite-specific errors, though in a less aggressive fashion than would be required without DCA. How much less is still a matter of investigation.

Improvements

Since accomplishment of the DCA solution and evaluation described herein, DCA has been expanded and improved. Recall that one preliminary observation was that the range of perigee altitudes was suspect, particularly at the low end where the inflection temperature corrections dominate. Analysis by AFSPC/ASAC found this indeed to be the case. DCA was not offering measurable improvement below about 300 km altitude, which corresponds to the lower boundary of the calibration and evaluation satellite sets.

Therefore, the calibration constellation was expanded by 16 satellites, all with perigees in the 200-300 km range. (All had significant eccentricities to remain in orbit for suitably long periods of time.) Also, one of the higher calibration satellites was dropped due to questionable performance, bringing the constellation to a total of 75 satellites. With this expanded constellation, significant improvements in the 150-300 km altitude range were realized without compromising the results contained herein. Moreover, a 1x1 field became feasible for the inflection temperature, with a 2×2 field still being retained for the exospheric temperature.

Finally, it was found that applying *a priori* information, to include autocorrelation via a first-order Markov process, could improve the DCA solution. Though this capability was available all along, it was not particularly feasible to use in the beginning of the study because it required statistical information on the various temperature coefficients not available then. While the resulting gain in epoch accuracy and ballistic coefficient consistency is relatively small, the solved-for temperature field is smoother and uniformly spaced at 3 hours, rather than having different parts of the field solved for at different resolutions. This is esthetically and practically preferable.

References

1. Jacchia, L. G.; "New Static Models of the Thermosphere and Exosphere with Empirical Temperature Profiles", Special Report 313, Smithsonian Astrophysical Observatory, May 1970.

2. Storz, Mark F.; "Modeling and Simulation Tool for the High Accuracy Satellite Drag Model", *AAS/AIAA Astrodynamics Specialist Conference* (Quebec City, Quebec, Canada), August 2001.